Phase Segregation of MnP in Chalcopyrite Dilute Magnetic Semiconductors: A Cautionary Tale

Jennifer A. Aitken,[†] Georgiy M. Tsoi,[‡] Lowell E. Wenger,[‡] and Stephanie L. Brock*[,§]

Department of Chemistry and Biochemistry, Duquesne University, Pittsburgh, Pennsylvania 15282, Department of Physics, University of Alabama at Birmingham, Birmingham, Alabama 35294, and Department of Chemistry, Wayne State University, Detroit, Michigan 48202

Received May 29, 2007. Revised Manuscript Received August 10, 2007

On the basis of reports of room-temperature ferromagnetism in Mn-doped semiconductor chalcopyrites, we undertook an investigation of a new doped system, $CdSnP_2$:Mn. $CdSnP_2$ heated with Mn powder in a tube furnace under flowing argon at 350 and 500 °C resulted in a material having ferromagnetic properties ($T_c \approx 290$ K) closely resembling those reported for other Mn-doped chalcopyrites (e.g., $CdGeP_2$, $ZnGeP_2$). However, the appearance of weak MnP impurity peaks in the powder X-ray diffraction pattern for the 500 °C prepared sample, coupled with the strong similarity in the measured ferromagnetic behaviors, suggests that the ferromagnetic response may not be an intrinsic effect. Measurements on bulk and nanocrystalline MnP as well as on control samples prepared by heating CdP_2 or red phosphorus with Mn powder lead to the conclusion that (i) heating mixtures of $CdSnP_2$ with Mn results in phase-segregated MnP, a room-temperature ferromagnetic material, and (ii) amounts as small as 0.3 wt % (1.0 mol %) MnP, well below the resolution of powder X-ray diffraction, are sufficient to dominate the magnetic response in these chalcopyrite materials.

1. Introduction

Dilute magnetic semiconductors (DMS) have attracted considerable interest over the past 30 years, as a variety of magnetic behaviors have been observed depending upon the magnetic element doped into the nonmagnetic semiconductor. Moreover, the electronic and/or optical properties of the semiconductor can even be changed or controlled if the magnetic concentration is sufficiently high to affect the carrier type and density. Thus, the opportunity exists in DMS for both electronic charge and spin degrees of freedom to be exploited for a variety of applications, especially if the DMS can be made to be ferromagnetic. In fact, the term "spintronics" [1,2] has become increasingly popular in describing devices that would make use of both the spin and charge of electrons in these semiconducting materials.

Among ferromagnetic DMS, the greatest attention has been focused on GaAs:Mn and InAs:Mn because these magnetically doped materials are chemically (and epitaxially) compatible with commercially employed semiconductors. This enables, for example, the formation of heterostructures for spin-injection.[3−5] Although the ferromagnetic interaction in these III−V semiconductors has been proven to be carrier-mediated[2] with ferromagnetic Curie temperatures as high 173 K,[6] doping at concentrations predicted to generate T_c values at or above room temperature, a prerequisite for practical devices, has proved difficult.[3,4,7] Indeed, attempts to introduce more than a few percent of Mn generally result in phase segregation of MnAs, and similar phase-segregation has been observed in other Mn-doped III−V semiconductors.[8,9] Although these heterogeneous materials exhibited ferromagnetic characteristics at room temperature, there is no evidence that the magnetic exchange is either promoted, or affected, by the carriers.

Considering the difficulties encountered in these binary systems, some groups have looked at doping ternary materials such as the semiconducting pnictides that adopt the chalcopyrite structure type: II−IV−V_2 (Figure 1). The room-temperature ferromagnetism recently reported in several Mn containing chalcopyrite materials, namely, $ZnGeP_2$:Mn,[10−14] $CdGeP_2$:Mn,[15−19] $MnGeP_2$,[20] $ZnGeAs_2$:Mn,[21] $CdGeAs_2$:

* To whom correspondence should be addressed. E-mail: sbrock@chem.wayne.edu.
[†] Duquesne University.
[‡] University of Alabama at Birmingham.
[§] Wayne State University.

(1) Wolf, S. A.; Awschalom, D. D.; Buhrman, R. A.; Daughton, J. M.; von Molnár, S.; Roukes, M. L.; Chtchelkanova, A. Y.; Treger, D. M. *Science* **2001**, *294*, 1488−1495.
(2) Ohno, H. *Science* **1998**, *281*, 951−956.
(3) Macdonald, A. H.; Schiffer, P.; Samarth, N. *Nat. Mater.* **2005**, *4*, 195−202.
(4) Schulthess, T. C.; Temmerman, W. M.; Szotek, Z.; Butler, W. H.; Stocks, G. M. *Nat. Mater.* **2005**, *4*, 838−844.
(5) Ohno, Y.; Young, D. K.; Beschoten, B.; Matsukura, F.; Ohno, H.; Awschaom, D. D. *Nature* **1999**, *402*, 790−792.
(6) Jungwirth, T.; Wang, K. Y.; Masek, J.; Edmonds, K. W.; Konig. J.; Sinova, J.; Polini, M.; Goncharuk, N. A.; MacDonald, A. H.; Sawicki, M.; Rushforth, A. W.; Campion, R. P.; Zhao, L. X.; Foxon, C. T.; Gallagher, B. L. *Phys. Rev. B* **2005**, *72*, 165204.
(7) Dietl, T.; Ohno, H.; Matsukura, F.; Cibert, J.; Ferrand, D. *Science* **2000**, *287*, 1019−1022.
(8) Laiho, R.; Lisunov, K. G.; Lähderanta, E.; Zakhvalinskii, V. S. *J. Phys. Condensed Matter* **1999**, *11*, 555−568.
(9) Cockayne, B.; MacEwan, W. R.; Harris, I. R.; Smith, N. A. *J. Cryst. Growth* **1985**, *73*, 637−640.
(10) Medvedkin, G. A.; Hirose, K.; Ishibashi, K.; Nishi, T.; Voevodin, V. G.; Sato, K. *J. Cryst. Growth* **2002**, *236*, 609−612.
(11) Baranov, P. G.; Goloshchapov, S. I.; Medvedkin, G. A.; Ishibashi, T.; Sato, K. *J. Superconductivity* **2003**, *16*, 131−133.
(12) Cho, S.; Choi, S.; Cha, G. −B.; Hong, S. C.; Kim, Y.; Zhao, Y. −J.; Freeman, A. J.; Ketterson, J. B.; Kim, B. J.; Kim, Y. C.; Choi, B.-C. *Phys. Rev. Lett.* **2002**, *88*, 257203.

10.1021/cm071454z CCC: $37.00 © 2007 American Chemical Society
Published on Web 10/05/2007

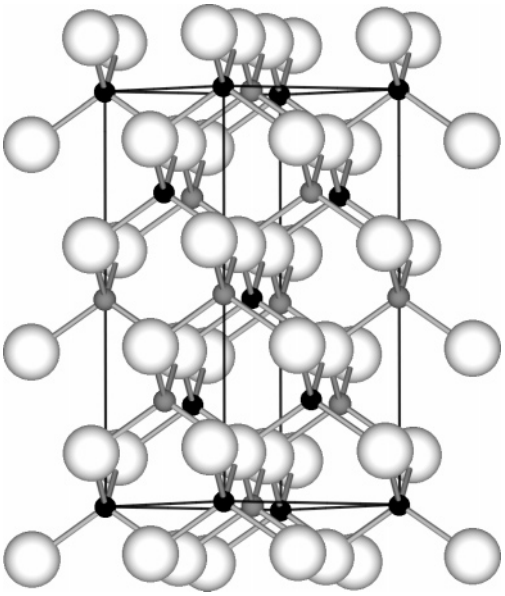

Figure 1. Chalcopyrite crystal structure of $CdSnP_2$ viewed down the crystallographic (100) direction. Filled black and gray spheres represent Cd and Sn sites, respectively. Large open spheres represent P.

Mn,[22,23] $MnGeAs_2$,[19] and $ZnSnAs_2$:Mn[24] has added to the interest in these materials. Although chalcopyrite materials are not routinely utilized in semiconductor applications, the close lattice matching with some III−V phases combined with the high ferromagnetic transition temperatures make them potential candidates for practical spintronic devices. However, the question of whether the magnetic response is carrier mediated (i.e., "spintronic") has yet to be addressed for these doped chalcopyrites.

In addition to the experimental reports, a number of theoretical calculations have been undertaken to understand the magnetism exhibited in these doped chalcopyrites. These calculations suggest an antiferromagnetic ground state for Mn substitution onto the divalent site in II−Ge−V_2 (II = Zn, Cd; V = P, As).[25−27] However, if Mn can be substituted onto the Ge site in $CdGeP_2$, or onto a mixture of Cd and Ge sites, a ferromagnetic ground state is favored.[28,29] A recent examination by Erwin[30] on a wide range of chalcopyrites suggests that although doping of Mn on the IV site of $CdGeP_2$ and $CdGeAs_2$ may give rise to ferromagnetism, similar doping of $ZnGeP_2$, $ZnGeAs_2$, and $ZnSnAs_2$ is expected to yield an antiferromagnetic ground state. Additionally, all of these phases are expected to have positive impurity formation energies for the IV site, which favors substitution on the II site and consequently an antiferromagnetic ground state.

In the study reported here, a potential new member of the DMS chalcopyrites, $CdSnP_2$:Mn, has been investigated. In investigating this new phase, care was taken to distinguish between the intrinsic magnetism of this doped chalcopyrite phosphide and that from a possible MnP impurity. The results indicate that the observation of ferromagnetism in this DMS arises from MnP formation (in bulk and/or nanoscale form) that occurs spontaneously under conditions commonly employed for synthesis of Mn-doped chalcopyrites.

2. Experimental Section

2.1. Synthesis. *2.1.1. Preparation of $CdSnP_2$.* $CdSnP_2$ crystals were prepared from a tin flux reaction. In an argon-filled glovebox, 0.3134 g of CdP_2 powder (99.9%, Cerac) and 7.4552 g of Sn metal shot (99.9%, Cerac) were loaded into an alumina crucible, which was subsequently inserted into a fused-silica ampule and sealed under a vacuum. The ampule was placed in a muffle furnace so that it stood vertically and was heated from room temperature to 650 °C at 100 °C/h, held at 650 °C for 24 h, followed by cooling at a rate of 2 °C/h to 450 °C and 3 °C/h to 200 °C, then rapidly to room temperature. The final product in the crucible was then stirred in a warm, dilute nitric acid solution to dissolve the excess tin metal. The resulting crystals were several millimeters long and did not appear to have any residual flux attached.

2.1.2. Preparation of $CdSnP_2$:Mn. Mn-doped $CdSnP_2$ samples were subsequently prepared by combining approximately 0.08 g of these $CdSnP_2$ crystals with 0.004 g of Mn (99.9%, Strem, cleaned with 10% HNO_3 in methanol) metal powder in a tube furnace. The finely ground mixture was placed into a 2 mL alumina boat and loaded into a fused-silica tube within the tube furnace. The mixture was then heated from room temperature to 350 or 500 °C under flowing argon over 1 h, held at final temperature for 1 h, and cooled to room temperature over 1 h.

2.1.3. Preparation of MnP. Bulk MnP was prepared by grinding 1.0467 g of Mn metal powder and 0.5978 g red P powder (EM Science) together and loading the mixture into a 12 mm i.d. carbon-coated, fused-silica tube. The tube was sealed under a vacuum and heated from room temperature to 1000 °C at a rate of 100 °C/day. Heating the Mn and red P powders more quickly results in an explosion, whereas not adding excess red phosphorus results in a manganese rich impurity phase in the sample, $Mn_{5.64}P_3$. The tube was held at 1000 °C for 4 days, followed by cooling to room temperature at a rate of 25 °C/h.

2.1.4. Preparation of $ZnSnP_2$:Mn. Although attempts to dope $CdSnP_2$ with Mn directly from a tin flux reaction of 0.2093 g of

(13) Cho, S.; Choi, S.; Cha, G. −B.; Hong, S. C.; Kim, Y.; Ketterson, J. B.; Kim, B. J.; Kim, Y. C.; Choi, B. -C.; Jeong, J. -H. *J. Korean Phys. Soc.* **2003**, *42*, S724−S726.
(14) Sato, K.; Medvedkin, G. A.; Ishibashi, T. *J. Cryst. Growth* **2002**, *237−239*, 1363−1369.
(15) Medvedkin, G. A.; Ishibashi, T.; Nishi, T.; Hayata, K.; Hasegawa, Y.; Sato, K. *Jpn. J. Appl. Phys.* **2000**, *39*, L949−L951.
(16) Sato, K.; Medvedkin, G. A.; Nishi, T.; Hasegawa, Y.; Misawa, R.; Hirose, K.; Ishibashi, T. *J. Appl. Phys.* **2001**, *89*, 7027−7029.
(17) Medvedkin, G. A.; Ishibashi, T.; Nishi, T.; Sato, K. *Semiconductors* **2001**, *35*, 291−294.
(18) Sato, K.; Medvedkin, G. A.; Ishibshi, T.; Nishi, T.; Misawa, R.; Yonemitsu, K.; Hirose, K. *J. Magn. Soc. Jpn.* **2001**, *25*, 735−738.
(19) Hirose, K.; Medvedkin, G. A;, Ishibashi, T.; Nishi, T.; Sato, K. *J. Cryst. Growth* **2002**, *237−239*, 1370−1373.
(20) Cho, S.; Choi, S.; Cha, G. -B.; Hong, S. C.; Kim, Y.; Freeman, A. J.; Ketterson, J. B.; Park, Y.; Park, H. M. *Solid State Commun.* **2004**, *129*, 609−613.
(21) Choi, S.; Choi, J.; Hong, S. C.; Cho, S.; Kim, Y.; Ketterson, J. B. *J. Korean Phys. Soc.* **2003**, *42*, S739−S741.
(22) Demin, R.; Koroleva, L.; Marenkin, S.; Mikhailov, S.; Aminov, T.; Szymczak, H.; Szymszak, R.; Baran, M. *J. Magn. Magn. Mater.* **2005**, *290−291*, 1379−1382.
(23) Storchak, V. G.; Eshchenko, D. G.; Luetkens, H.; Morenzoni, E.; Lichti. R. L.; Marenkin, S. F.; Pashkova, O. N.; Brewer, J. H. *Phys. B: Condensed Matter* **2006**, *374*, 430−432.
(24) Choi, S.; Cha, G.-B.; Hong, S. C.; Cho, S.; Kim, Y.; Ketterson, J. B.; Jeong, S.-Y.; Yi, G.-C. *Solid State Commun.* **2002**, *122*, 165−167.
(25) Zhao, Y.-J.; Geng, W. T.; Freeman, A. J.; Oguchi, T. *Phys. Rev. B* **2001**, *63*, 201202.
(26) Picozzi, S.; Continenza, A.; Zhao, Y.-J.; Geng, W.-T.; Freeman, A. J. *J. Vac. Sci. Technol., A* **2002**, *20*, 2023−2026.
(27) Freeman, A. J.; Zhao, Y.-J. *J. Phys. Chem. Solids* **2003**, *64*, 1453−1459.
(28) Mahadevan, P.; Zunger, A. *Phys. Rev. Lett.* **2002**, *88*, 047205.
(29) Mahadevan, P.; Zunger, A. *Phys. Rev. Lett.* **2002**, *88*, 159904.
(30) Erwin, S. C.; Zutic, I. *Nat. Mater.* **2004**, *3*, 410−414.

Cd (99.999%, Cerac), 0.0114 g of Mn, 0.1275 g of red P, and 8.1868 g of Sn metal shot were unsuccessful, the preparation of Mn-doped $ZnSnP_2$ crystals was achieved by reacting 0.0914 g of Zn (99.999%, Cerac), 0.0085 g of Mn, 0.0962 g of P, and 3.4655 g of Sn. The mixture was loaded into an alumina crucible, placed in a fused-silica tube, and heated, with the product being isolated in the same manner as described for $CdSnP_2$.

2.1.5. Preparation of Control Samples. The reactivity of Mn with CdP_2 was probed by heating a finely ground mixture containing 0.0306 g of CdP_2 with 0.0017 g of Mn at 350 °C under flowing Ar for 1 h. The corresponding reactivity of Mn metal and red phosphorus was determined by heating a finely ground mixture with a 1:1 Mn:P molar ratio at 350 °C under flowing Ar for 1 h.

2.2. Physical Measurements. *2.2.1. Powder X-ray Diffraction (PXRD).* PXRD patterns were collected with a Rigaku RU200B rotating anode powder X-ray diffractometer operating at 40 kV and 150 mA using graphite-monochromatized Cu Kα radiation. Samples were ground with a mortar and pestle and deposited onto a glass slide coated with a thin layer of petroleum jelly. $\theta-2\theta$ scans were performed from 10 to 70° with a speed of 0.1°/min. Crystalline phases were identified using the search match capabilities of the JADE program along with the ICDD (International Center for Diffraction Data) powder diffraction file (PDF) database. Lattice parameter refinements using the program CELREF[31] were determined from PXRD patterns on the powders both before and after the experiment, using silicon powder as a standard reference.

2.2.2. Magnetization Studies. DC magnetization studies were performed using a Quantum Design model MPMS-5S SQUID magnetometer. Temperature-dependent magnetization was acquired from 5 to 300 K in an applied field of 5.0 kOe. Samples were cooled in a field (5 kOe) or in zero field prior to measurements conducted from low to high temperatures at 5 kOe. Magnetization-vs-magnetic field measurements were obtained at 5, 50, 150, and 300 K. In all cases, samples were sealed in ca. 15 cm long fused-silica tubes under a vacuum in order to prevent any possible oxidation of the powders while the magnetic measurements were performed.

2.2.3. Inductively Coupled Plasma−Mass Spectrometry (ICP−MS). Quantitative analyses of Cd, Sn, P, and Mn were performed by RTI Laboratories, Inc. (Livonia, MI), using ICP−MS. Samples were prepared by dissolution in a 10% aqua regia solution.

3. Results and Discussion

In the present work, Mn-doping in $CdSnP_2$ was investigated by a substitution method developed by Sato and coworkers,[14] in which undoped chalcopyrite single crystals or polycrystalline powder is combined with elemental Mn and heated in a tube furnace under flowing gas. Crystals of $CdSnP_2$, presynthesized using a Sn-flux, were ground with manganese (4.5−4.9 wt %) and then heated in a tube furnace under argon gas at 350 or 500 °C for 1 h. Powder X-ray diffraction peaks of the 350 °C prepared sample were indexed to $CdSnP_2$ and Sn metal (Figure 2a). Even though there is no discernible change in the chalcopyrite lattice parameters, ICP−MS analysis on the resulting recovered material does confirm the presence of Mn (4−8% by weight). In comparison, other groups have reported nearly a 1% decrease in the lattice parameters upon Mn incorporation in $CdGeP_2$[16,19] and a 0.34% increase in the unit-cell volume for $Zn_{0.944}Mn_{0.056}GeP_2$[12] relative to the undoped phase, both of which are consistent with expectations based on the relative size of the native and dopant ions. In the case of Mn-doped $ZnSnAs_2$, a decrease in lattice constants of 0.063% has been reported.[24] However, because Mn replacement for Zn should result in an increase in the lattice constants on the basis of Vegard's Law, the possibility of Mn substitution on both the II and IV sites was proposed. Alternatively, doping at interstitial sites or the presence of inadvertently incorporated codopants may explain the variances.

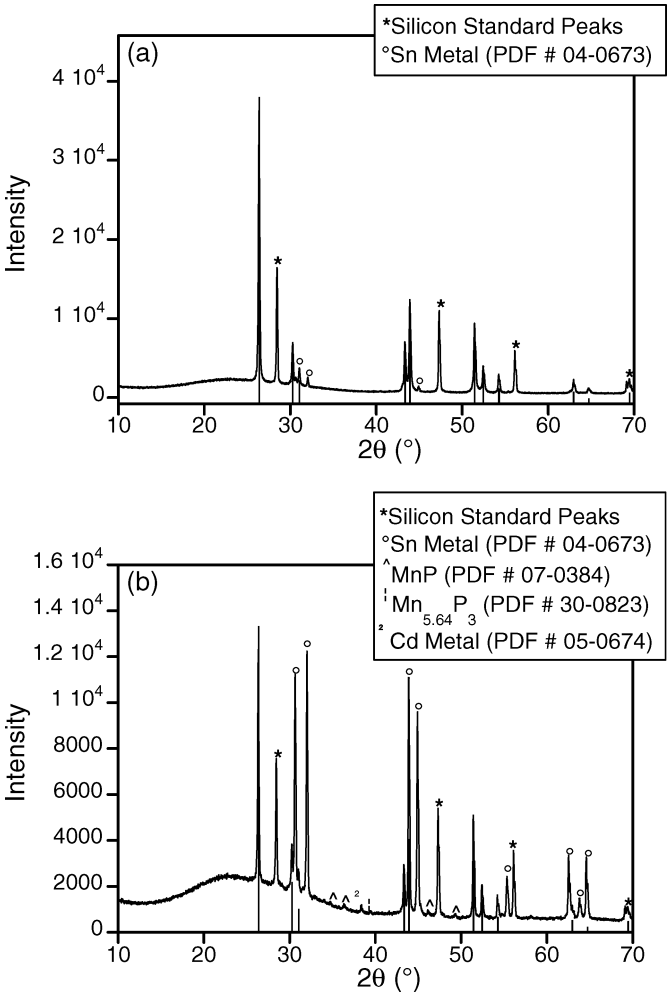

Figure 2. Powder X-ray diffraction pattern obtained for (a) $CdSnP_2$ + Mn heated to 350 °C in flowing Ar; (b) $CdSnP_2$ + Mn heated to 500 °C in flowing Ar. The line diagram at the bottom of each graph corresponds to the powder diffraction file (PDF) for $CdSnP_2$ (#73-0400).

Consistent with results on other Mn-doped chalcopyrites, the magnetization data suggest that $CdSnP_2$:Mn samples prepared at 350 °C are ferromagnetic (Figures 3a and 4a). The onset of ferromagnetic behavior occurs around 315 K with a ferromagnetic Curie temperature, T_c, of 290 K (as determined from the maximum in the first derivative of the temperature-dependent magnetization) and a room-temperature coercivity of approximately 0.2 kOe. These values are in surprisingly close quantitative agreement with those reported on the other chalcopyrite phosphide systems, where the onset of ferromagnetism, typically reported as T_c, occurs in the 300−320 K region and room-temperature coercivities range from 0.22 to 0.84 kOe for a wide range of dopant concentrations.[10,12−14,19] Below 50 K, a bifurcation between

(31) Laugier, J.; Bochi, B. *CELREF Program*; Laboratoire des Matèriaux du Genie Physique: Saint Martin d'Hères, France.

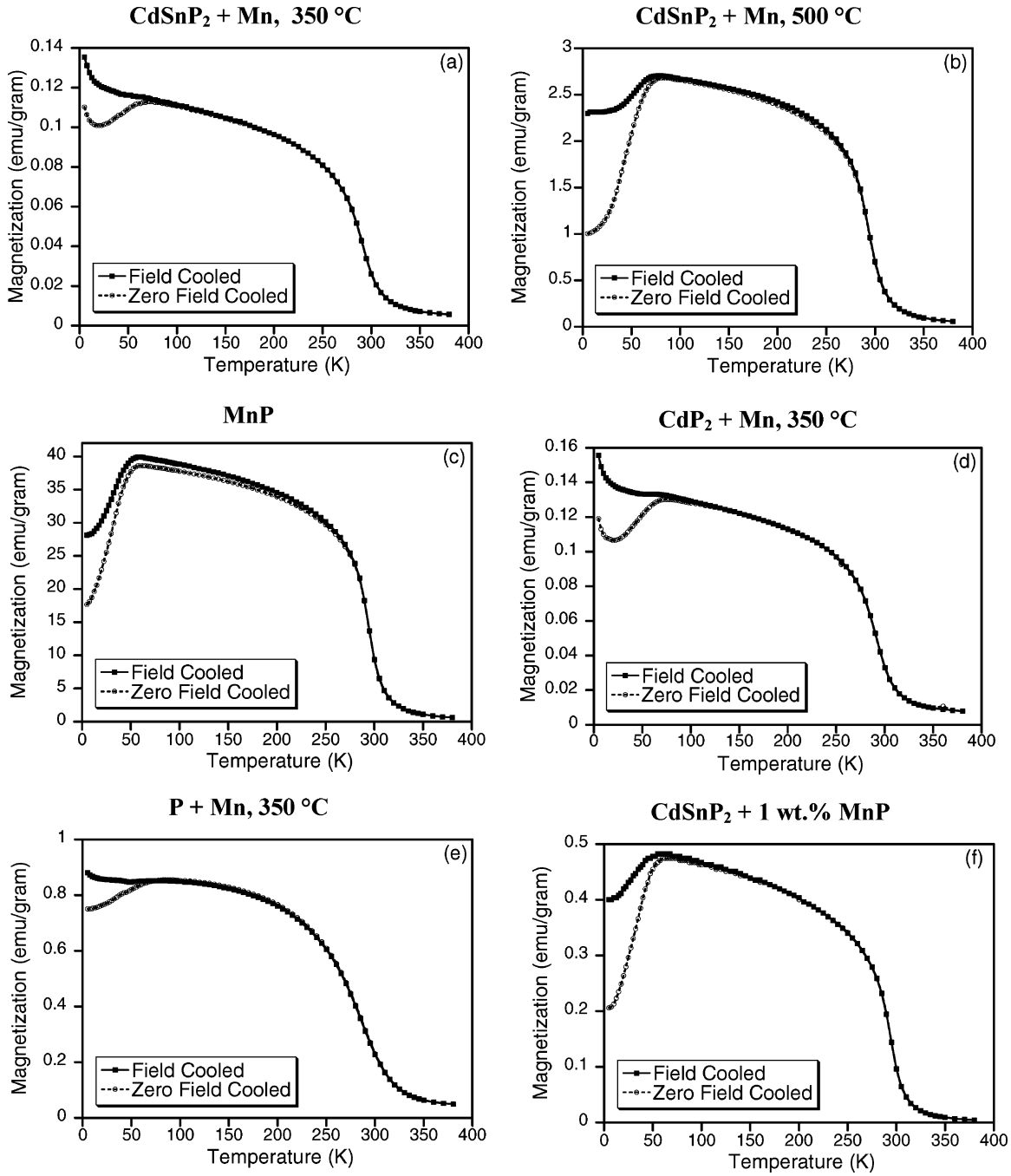

Figure 3. Temperature dependence of the mass magnetization in a magnetic field of 5.0 kOe for (a) $CdSnP_2$ + Mn heated to 350 °C; (b) $CdSnP_2$ + Mn heated to 500 °C; (c) MnP; (d) CdP_2 + Mn heated to 350 °C; (e) P + Mn heated to 350 °C; (f) physical mixture of $CdSnP_2$ + 1 wt % MnP.

the field-cooled (FC) and zero-field-cooled (ZFC) magnetizations occurs followed by a paramagnetic upturn at the lowest temperatures (Figure 3a). This upturn is also manifested in the magnetization vs field data at 5 K as the magnetization continues to increase as a function of magnetic field, instead of saturating at the highest field values (Figure 4a).

The temperature-dependent magnetizations for $CdSnP_2$:Mn prepared at 500 °C (Figure 3b) are very similar to those of the 350 °C prepared sample (Figure 3a), except that for the 500 °C prepared sample the magnitude of the magnetization is an order of magnitude larger and the low-temperature paramagnetic upturn is not as readily apparent. In addition, the magnetic hysteresis at 5 K for the 500 °C prepared sample (Figure 4b) is much wider (larger coercive field) than that measured for the 350 °C sample (Figure 4a) and shows a distinct kinklike structure in the vicinity of 2−3 kOe. This strangely shaped hysteresis has also been reported in some other chalcopyrite systems, most notably in $ZnGeP_2$:Mn samples[12] prepared at 1100 °C for relatively high Mn concentrations (5.6% substitution of Mn for Zn), and has been ascribed to the presence of an antiferromagnetic ground state at low temperatures, as predicted from various computational studies.[25−30] However, the PXRD pattern for the 500 °C prepared sample (Figure 2b) not only displays peaks associated with the $CdSnP_2$ phase and Sn metal, but several other peaks, including some barely detectable ones, that can be indexed to MnP.

To determine to what extent the presence of crystalline MnP, as detected by PXRD, could be contributing to the

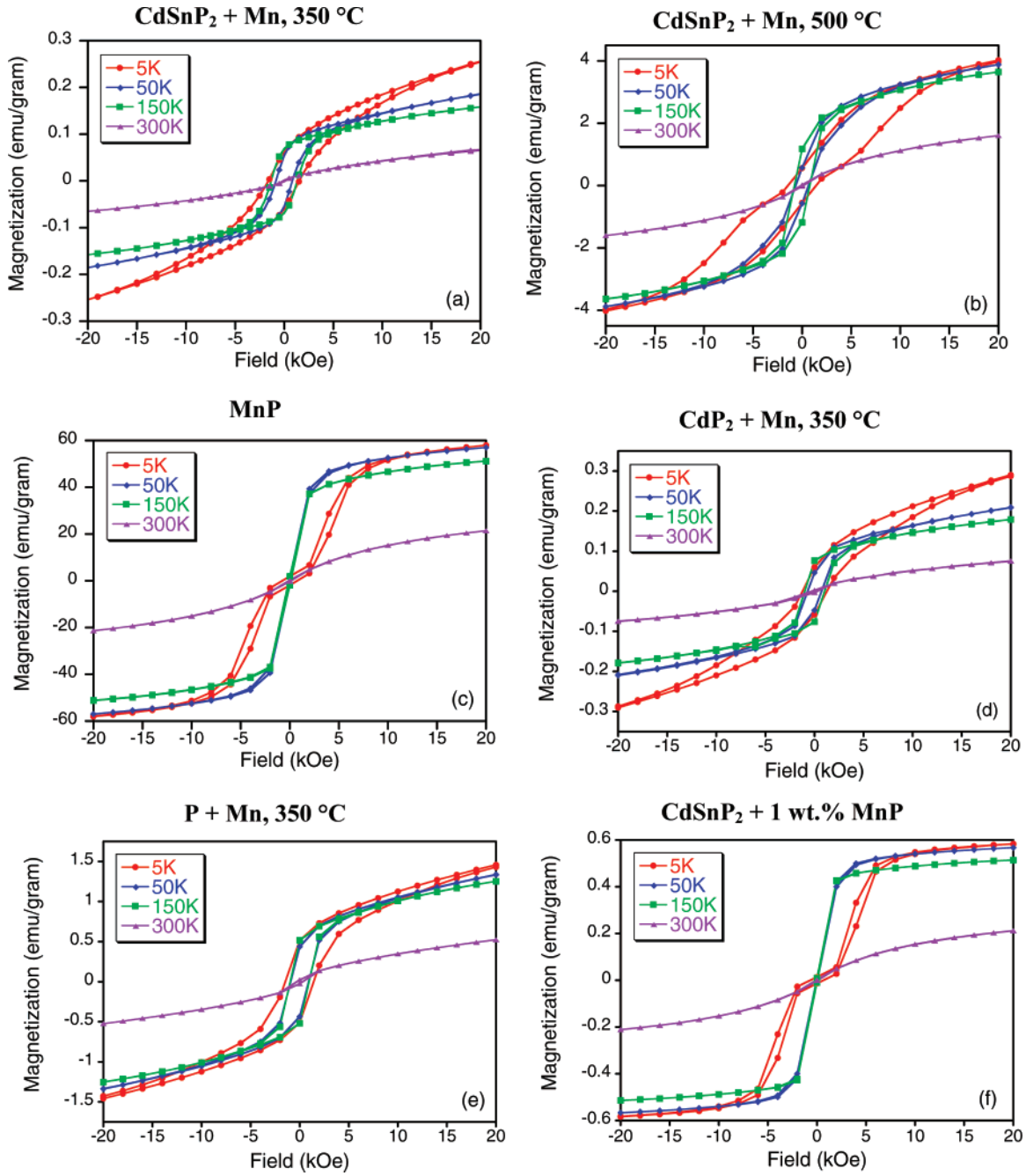

Figure 4. Magnetic field dependence of the mass magnetization for (a) $CdSnP_2$ + Mn heated to 350 °C; (b) $CdSnP_2$ + Mn heated to 500 °C; (c) MnP; (d) CdP_2 + Mn heated to 350 °C; (e) P + Mn heated to 350 °C; (f) a physical mixture of $CdSnP_2$ + 1 wt % MnP.

observed magnetic response in the 500 °C prepared sample, measurements of the magnetic properties of bulk MnP were undertaken for comparison. The temperature-dependent magnetization of polycrystalline MnP (Figure 3c) exhibits an archetypal behavior associated with a bulklike ferromagnetic ordering with the transition occurring at 290 K, in agreement with the reported T_c value for single-crystal MnP.[32] Below ~50 K, however, the ZFC and FC magnetization curves slope downward because of the transition from the ferromagnetic state to a metamagnetic state in accordance with previous work on MnP. This metamagnetic state is also characterized by the appearance of a kink in the S-shaped magnetic hysteresis acquired at 5 K (Figure 4c). At 50 K and above, the M vs H curves are anhysteretic (not coercive) with a saturation magnetization value of ~60 emu/g. Although the saturated magnetization measured for this polycrystalline MnP sample is about 30% smaller than that reported on single-crystal MnP,[30] this value is reasonable considering that the magnetization of MnP is highly anisotropic. Obviously, the strong similarity in magnetization characteristics of bulk MnP with that of the 500 °C prepared $CdSnP_2$:Mn sample, particularly the presence of a kink in the hysteresis loops observed below 50 K, suggests that a significant part of the ferromagnetic response in the 500 °C prepared sample is due to the presence of MnP.

Although many of the qualitative magnetic features are similar between bulk MnP and the 350 °C prepared $CdSnP_2$:Mn sample, several distinct differences are observed for this

(32) Huber, E. E., Jr.; Ridgley, D. H. *Phys. Rev.* **1964**, *135*, A1033−A1040.

doped sample, including the absence of any kink in the S-shaped magnetic hysteresis below 50 K, the finite coercivity values and magnetic hystereses above 50 K, the less distinctive temperature-dependent ZFC and FC magnetizations that are typically associated with the metamagnetic transition below 50 K, and the appearance of a paramagnetic feature at the lowest temperatures. Although it is possible that these differences arise from the presence of a doped semiconductor phase, the most straightforward answer is that magnetic properties arise from a combination of MnP nanoparticles and a small amount of another paramagnetic entity.

As has been recently reported, MnP nanoparticles[33,34] indeed order ferromagnetically just below 300 K, similar to bulk MnP. However, the magnetization behaves differently from bulk MnP below 50 K as the magnetic hysteretic behavior remains S-shaped with no kink and exhibits relatively large coercivities of 4−6 kOe. Also, the ZFC and FC magnetizations at low applied fields are reminiscent of a superparamagnet around its blocking temperature, with the temperature of the bifurcation between the ZFC and FC magnetizations exhibiting a clear dependence on the particle volume. In short, the metamagnetic phase is completely destabilized in MnP nanoparticles and the resulting magnetic characteristics are actually quite similar to those of the 350 °C prepared $CdSnP_2$:Mn sample.

Although these observations suggest that the ferromagnetic behavior arises from MnP nanoparticles, the question remains as to whether nanocrystalline MnP can actually be formed from the reaction of elemental Mn with a phosphide at the relative low temperature of 350 °C. To determine this, we undertook reactions between CdP_2 and Mn and between red phosphorus and Mn under identical conditions to the 350 °C prepared chalcopyrite sample. Although neither the reaction with CdP_2 nor with red phosphorus show any sign of MnP formation by powder X-ray diffraction, the magnetization results (Figures 3d, 3e, 4d, and 4e) for the reacted materials are similar in behavior to those of the $CdSnP_2$:Mn sample heated at 350 °C, including their Curie temperatures of 291 K. This leaves little doubt that the ferromagnetic behavior in the Mn-doped $CdSnP_2$ is due to MnP formation.

The possibility of MnP formation is perhaps not too surprising, as these reactions in a tube furnace with flowing gas that are employed for doping the II−IV−V_2 chalcopyrites have a number of drawbacks. First, they rely on elemental Mn displacing a divalent (e.g., Cd^{2+}) or tetravalent (e.g., Ge^{4+}) cation thermally, presumably with a concomitant reduction of these species as Mn is ionized. Then, the displaced species needs to be lost by vapor transport. Second, this Mn displacement, even in single crystals, is not necessarily uniformly distributed throughout the sample,[15,17,19] which could lead to MnP-rich nanocrystalline regions. In an initial effort to avoid the potential complications of the elemental exchange route, while maintaining relatively low temperatures to minimize MnP formation, Sn-flux reactions were attempted at 650 °C in which Mn was directly incorporated into the molten metal reaction with a proportional decrease in the quantity of Cd metal. However, no manganese was detected in these samples by ICP analyses, and all samples showed diamagnetic behavior with a small paramagnetic upturn in the magnetization at low temperatures.

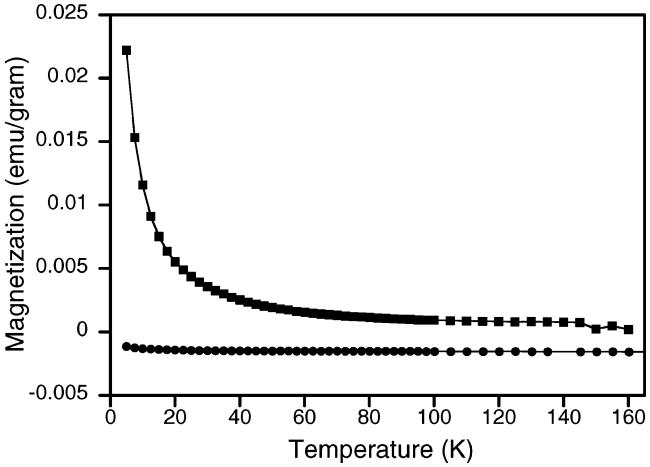

Figure 5. Temperature dependence of the mass magnetization for undoped $ZnSnP_2$ (circles) and Mn-doped $ZnSnP_2$ (squares) prepared via a Sn-flux reaction.

Presuming that homogeneous doping might be facilitated for similar-sized divalent ions, we prepared undoped and Mn-doped $ZnSnP_2$ crystals following a similar flux-reaction strategy. Although $Zn_{0.9}Mn_{0.1}SnP_2$ was targeted (2.2 wt % Mn), ICP results indicate that the doped sample contained only 0.084 wt % Mn. Magnetically, although the undoped $ZnSnP_2$ sample displayed a diamagnetic behavior with a barely perceptible paramagnetic upturn at the lowest temperatures, the temperature-dependent magnetization for the $ZnSnP_2$:Mn sample exhibited a paramagnetic behavior at all temperatures (Figure 5) with no indication of any ferromagnetic characteristics. An effective Mn moment of about 3.5 ± 0.5 Bohr magnetons was determined from the Curie-like paramagnetic behavior, which is about 60% of the normal value found for Mn^{2+} ions. The appearance of this paramagnetic behavior in this Mn-doped $ZnSnP_2$ sample, in combination with the observation of a paramagnetic-like behavior at the lowest temperatures for the Mn-doped $CdSnP_2$ sample, suggests that this may be the intrinsic property of this DMS with Mn acting as a paramagnetic ion dopant. Unfortunately, the magnetization data cannot distinguish whether this behavior results from paramagnetic Mn ions being located on substitutional sites of the chalcopyrite crystal structure or on interstitial sites, or from some other Mn impurity phase formed during the synthesis process.

Is it reasonable to assume that small amounts of nanocrystalline, or even bulk, MnP would not be detected by powder X-ray diffraction, yet have such a dramatic effect on the magnetic response? To address this question, a physical mixture of $CdSnP_2$ with 1 wt % MnP (3.3 mol %) powder was made. Although no peaks associated with the addition of 1 wt % MnP could be detected in the PXRD spectrum, one can clearly see from comparison of the temperature-dependent magnetization (panels c and f in

(33) Perera, S. C.; Tsoi, G.; Wenger, L. E.; Brock, S. L. *J. Am. Chem. Soc.* **2003**, *125*, 13690−13691.
(34) Gregg, K. A.; Perera, S. C.; Lawes, G.; Shinozaki, S.; Brock, S. L. *Chem. Mater.* **2006**, *18*, 879−886.

Figure 3) and the field-dependent magnetization (panels c and f in Figure 4) that the magnetization results for the physical mixture of MnP with $CdSnP_2$ are identical to that obtained for bulk MnP after scaling for the 1:100 mass ratio. Thus, the appearance of MnP peaks in the PXRD spectra for the 500 °C prepared sample, and their absence in the 350 °C prepared sample, is consistent with respect to the relative magnitudes of the magnetization measured for these Mn-doped samples and the 1 wt % MnP control sample. Assuming that the magnetization measured for the 500 °C prepared sample is entirely due to MnP, the equivalent of approximately 6−7 wt % MnP is needed for detection by powder X-ray diffraction. Similarly, the magnetic response from as little as 0.3 wt % MnP in $CdSnP_2$ would result in a magnetization comparable to that measured for the 350 °C prepared sample. It should be further noted that if the magnetic response in these $CdSnP_2$:Mn samples arises from MnP nanoparticulates, as surmised here, the detection of the MnP phase in powder X-ray diffraction studies would be even more challenging, because a nanocrystalline phase would exhibit broad diffraction peaks.

4. Conclusion

In summary, the present study shows that (1) quantities of bulk-phase MnP well below the detection limit of powder X-ray diffraction can still dominate the magnetic response of a material. In comparison, the majority of previous reports on Mn-doped chalcopyrites argue against MnP as a magnetic impurity on the basis of the absence of the peaks in the powder X-ray diffraction pattern. (2) The characteristic ferromagnetic behavior (onset at $T = 315$ K) and the Curie temperature ($T_c = 290$ K) for MnP are virtually identical to the ferromagnetic behavior and onset temperature observed for our Mn-doped $CdSnP_2$ samples prepared at 350 and 500 °C, as well as for the control reactions of CdP_2 + Mn and red phosphorus + Mn at 350 °C. The similarity with the onset/T_c values reported for other chalcopyrites doped with various Mn concentrations would not be expected, because ferromagnetic order arising from magnetic exchange or carrier-mediated coupling should result in higher T_c values with increasing Mn concentration. Furthermore, recent NMR studies[35] on bulk polycrystalline $Zn_{1-x}Mn_xGeP_2$ also report that the ferromagnetism in these materials is attributable to MnP, which supports this extrinsic effect conclusion. (3) The difference in the low-temperature magnetic behavior in $CdSnP_2$:Mn from that of bulk MnP, including the presence of magnetic hystereses, can be attributed to nanocrystalline MnP, which can form at temperatures as low as 350 °C. Samples prepared at higher temperatures will naturally lead to larger MnP phase-segregated regions and the observation of more bulklike MnP behavior, such as a kink in the magnetic hysteresis curve typically associated with the metamagnetic state of bulk MnP. (4) The intrinsic magnetic property for doped chalcopyrites may be paramagnetic, such as is observed for $ZnSnP_2$:Mn. However, the ferromagnetic response from even small amounts of MnP does not permit one to distinguish whether the low-temperature magnetic behavior is an intrinsic effect or due to some other paramagnetic impurity.

In any system where doping occurs at very low levels, distinguishing whether magnetic effects are intrinsic, or due to phase segregation, is complicated. The present study joins a handful of others suggesting that some of the reported room-temperature ferromagnetic semiconductors may result from phase segregation and that more careful materials characterization may be necessary.[36−39] Finally, although the corresponding arsenide phases have not been investigated in this study, similar caution should be taken in ascertaining whether the ferromagnetism observed in the Mn-doped arsenide chalcopyrites is intrinsic or arises from MnAs, which has a first-order ferromagnetic transition at 317 K with an onset near 323 K in unstrained samples.[40,41] With the introduction of strain, as occurs when MnAs nanocrystals are embedded in GaAs, the ferromagnetic transition shifts to higher temperatures (∼330 K),[42,43] a temperature that is comparable to the T_c values reported for Mn-doped arsenide chalcopyrites (329−355 K).[20−24]

Acknowledgment. This work was supported in part by the Wayne State University Institute of Manufacturing Research and the National Science Foundation (Career Award, DMR-0094273).

CM071454Z

(35) Hwang, T.; Shim, J. H.; Lee, S. *Appl. Phys. Lett.* **2003**, *83*, 1809−1811.
(36) Kundaliya, D. C.; Ogale, S. B.; Lofland, S. E.; Dhar, S.; Metting, C. J.; Shinde, S. R.; Ma, Z.; Barughese, B.; Ramanujachary, K. V.; Salamanca-Riba, L.; Venkatesan, T. *Nat. Mater.* **2004**, *3*, 709−714.
(37) Park, J. H.; Kim, M. G.; Jang, H. M.; Ryu, S.; Kim, Y. M. *Appl. Phys. Lett.* **2004**, *84*, 1338−1340.
(38) Lawes, G.; Risbud, A. S.; Ramirez, A. P.; Seshadri, R. *Phys. Rev. B* **2005**, *71*, 045201.
(39) Ando, K. *Science* **2006**, *312*, 1883−1885.
(40) Goodenough, J. B.; Kafalas, J. A. *Phys. Rev.* **1967**, *157*, 389−395.
(41) Tilsley, M. E. G.; Smith, N. A.; Cockayne, B.; Harris, I. R.; Lane, P. A.; Oliver, P. E.; Wright, P. J. *J. Alloys Compds.* **1997**, *248*, 125−131.
(42) Moreno, M.; Jenichen, B.; Däweritz, L.; Ploog, K. H. *Appl. Phys. Lett.* **2005**, *86*, 161903.
(43) Iikawa, F.; Brasil, M. J. S. P.; Adriano, C.; Couto, O. D. D.; Giles, C.; Santos, P. V.; Daweritz, L.; Rungger, I.; Sanviot, S. *Phys. Rev. Lett.* **2005**, *95*, 077203.